Available online at www.sciencedirect.com
ScienceDirect
Journal of Power Sources 178 (2008) 48–52
JOURNAL OF POWER SOURCES
www.elsevier.com/locate/jpowsour

Short communication

A novel binary Pt_3Te_x/C nanocatalyst for ethanol electro-oxidation

Meihua Huang, Fei Wang, Lirong Li, Yonglang Guo *

College of Chemistry and Chemical Engineering, Fuzhou University, Fuzhou 350002, PR China

Received 16 November 2007; received in revised form 10 December 2007; accepted 11 December 2007
Available online 26 December 2007

Abstract

The Pt_3Te_x/C nanocatalyst was prepared and its catalytic performance for ethanol oxidation was investigated for the first time. The Pt_3Te/C nanoparticles were characterized by an X-ray diffractometer (XRD), transmission electron microscope (TEM) and energy dispersive X-ray spectroscopy equipped with TEM (TEM-EDX). The Pt_3Te/C catalyst has a typical fcc structure of platinum alloys with the presence of Te. Its particle size is about 2.8 nm. Among the synthesized catalysts with different atomic ratios, the Pt_3Te/C catalyst has the highest anodic peak current density. The cyclic voltammograms (CV) show that the anodic peak current density for the Pt_3Te/C, commercial PtRu/C and Pt/C catalysts reaches 1002, 832 and 533 A g^{-1}, respectively. On the current–time curve, the anodic current on the Pt_3Te/C catalyst was higher than those for the catalysts reported. So, these findings show that the Pt_3Te/C catalyst has uniform nanoparticles and the best activity among the synthesized catalysts, and it is better than commercial PtRu/C and Pt/C catalysts for ethanol oxidation at room temperature.

Keywords: Anodic catalyst; Ethanol oxidation; PtTe/C; Tellurium

1. Introduction

The need for more efficient energy conversion is evident as the world fossil fuel sources become scarcer and the cost of them rises. Moreover, the urgent necessity of reducing the pollution in large urban centers promotes the use of non-polluting fuels, like hydrogen and renewable primary fuels in large scales [1]. Fuel cells have shown to be an interesting and very promising alternative to solving the problem of clean electric power generation with high efficiency. Fuel cells employing alcohols directly (direct alcohol fuel cell, DAFC) are attractive as power sources for mobile, stationary and portable applications. Compared with hydrogen-fed fuel cells, which need a reforming system and have problems of hydrogen storage, DAFCs use a liquid fuel, thus simplifying the fuel reforming and delivery system [2,3]. Methanol has been considered as the most promising fuel because it is more efficiently oxidized than other alcohols. But methanol is toxic and its crossover through the membrane also reduces the efficiency [4–6]. So ethanol as the direct fuel offers an attractive alternative because it is much less toxic than methanol and can be produced in large quantities from biomass, and its crossover is less than methanol [7]. Compared to methanol, ethanol has higher energy density (8.01 kWh kg^{-1} versus 6.09 kWh kg^{-1}). At the same time, the use of bioethanol will not change the natural balance of carbon dioxide in the atmosphere, in contrast with the use of fossil fuels [8].

Pt has been shown to be only an active and stable single metal catalyst for dissociative chemisorption of ethanol in acidic media [9]. However, Pt is readily poisoned by reaction intermediates such as CO and becomes inactive for completing the oxidation of ethanol to CO_2 in the potential region of fuel cell interest. But this ability for completing the oxidation of ethanol to CO_2 is necessary to break the C–C bond [10,11]. The high cost of the platinum also limits its use. Fortunately, it is found that addition of other metals to Pt can mitigate poisoning, increase the catalytic activity of Pt and reduce the cost [11]. To date, PtRu electrocatalyst is the best material for the anodic oxidation of ethanol from the viewpoint of current density, although some contradictory results can be found in the literature [3,12–14]. However, its complete oxidation to CO_2 is more difficult than that of methanol due to the difficulties in C–C bond breaking

* Corresponding author. Tel.: +86 591 8789 2893; fax: +86 591 8789 2893.
E-mail address: yguo@fzu.edu.cn (Y. Guo).

0378-7753/$ – see front matter © 2007 Elsevier B.V. All rights reserved.
doi:10.1016/j.jpowsour.2007.12.056

and the formation of CO-intermediates that poison the platinum-based anode catalysts [15,16].

It has been confirmed that the alcohol electro-oxidation in alkaline solutions is much less influenced by the reaction intermediates. However, alkaline aqueous solutions are not stable for DAFC owing to the carbonation [17]. It is well known that the DEFC is operating with a proton exchange membrane and the catalysts are in the acidic environment. Yet most metals and their oxides used for ethanol oxidation were dissoluted in acidic media [18]. Thus, for DEFC to be economically viable, a great effort has been devoted to the development of fuel cell electrocatalysts with the aims of increasing their activity and stability in acidic media and reducing the noble metal loading.

In this report, Te as a non-metallic element is used, for the first time, to prepare the Pt-based binary electrocatalyst because of its cheapness and good stability in acidic solutions (such as H_2SO_4, HCl, and $HClO_4$ solutions). And the characteristics of Pt_3Te_x/C nanocatalyst and its electrochemical behaviour were studied.

2. Experimental

Three milliliter $H_2PtCl_6{\cdot}6H_2O$ glycol solution (16.7 mM) was mixed with 20 ml glycol, 5 ml H_2O, 4.5 mg $Na_2TeO_4{\cdot}2H_2O$ and 36.7 mg Vulcan XC-72 carbon in a round flask. Then the mixture was treated in an ultrasound bath for 20 min and refluxed in an oil bath at 90 °C for 4 h in N_2 atmosphere. The excessive formic acid dissolved in glycol was added to the mixture to reduce Pt^{6+} and Te^{6+} completely. Finally, the mixture was washed with double-distilled water and dried at 85 °C for 8 h in a vacuum oven. The platinum nominal loading of the catalyst is 20 wt.% and the nominal atomic ratio of Pt to Te is 3:1. And with the same procedure, the $Pt_3Te_{1.5}$/C, $Pt_3Te_{0.5}$/C and Pt/C were synthesized.

The catalyst ink was prepared by mixing the catalyst in the isopropyl alcohol with a perfluorsulfonic acid solution (15 wt.% Nafion® solution) ultrasonically. Before use, the glassy carbon electrode was polished and rinsed ultrasonically with double-distilled water. The slurry was spread on a glassy carbon disk electrode as the working electrode (electrode area 0.1256 cm^2). Then the electrode was dried at 80 °C and it has 0.2 mg cm^{-2} Pt loading. A piece of Pt foil of 1 cm^2 was used as the counter electrode. Mercury sulfate electrode (MMS) was used as the reference one (0.62 V versus SHE). Before experiments, the 1.0 M CH_3CH_2OH + 0.5 M H_2SO_4 solution or 0.5 M H_2SO_4 solution were purged with ultrapure nitrogen gas for 20 min to expel oxygen. For comparative purposes, commercial carbon supported Pt and PtRu catalysts from Johnson Matthey Corporation (20 wt.%, molar ratio of Pt:Ru is 1:1) were used.

Characterizations of the catalyst nanoparticles were carried out by Philip X'Pert Pro MPP X-ray powder diffractometer (XRD) using a Cu Kα radiation (λ = 1.5418 Å) at a scan rate of 4° min^{-1} with step of 0.02°. The scan range was from 5° to 90°. The catalyst morphology and its elemental analysis were investigated by JEOL JEM-1010 Transmission Electron Microscope (TEM) working at 200 kV. Electrochemical measurements were carried out in a conventional three-compartment cell. Cyclic voltammograms (CV) were obtained in a potential range of −0.6 to 0.6 V at a scan rate of 50 mV s^{-1} using a CHI611B electrochemical working station (CH Instrument, Inc.). Due to slight contamination, the working electrode was cycled at 50 mV s^{-1} until a stable CV response was obtained in the 0.5 M H_2SO_4 solution. In all experiments, analytical grades and double-distilled water were used and the test electrolyte cell was in a water bath at 25 ± 0.2 °C.

3. Results and discussion

Fig. 1 shows the XRD spectra of synthesized Pt_3Te/C and commercial Pt/C catalysts. The diffraction peak at about 25° is corresponding to the (0 0 2) plane of the hexagonal structure of Vulcan XC-72 carbon. The characteristic diffraction peaks of Pt are clearly recognized at about 39°, 46°, 68° and 81° corresponding to Pt (1 1 1), (2 0 0), (2 2 0) and (3 1 1) plane, respectively. The Pt lattice parameter of 3.939 Å for the Pt_3Te/C catalyst is larger than that of 3.918 Å for the commercial Pt/C [19]. The result indicates that the addition of Te has some effect on the crystal lattice of Pt. No peaks of non-metallic Te or Te oxides were detected in the Pt_3Te/C catalyst, but their presence cannot be discarded because they may be present in an amorphous form. The average particle size for the Pt_3Te/C catalyst was estimated from the XRD peak of the (2 2 0) plane by using Sherrer's formula and was 2.4 nm [20].

Fig. 2 shows TEM image of the Pt_3Te/C catalyst. In TEM image, most of Pt_3Te/C particles are uniform and highly dispersed on the surface of carbon black. It should be noted that Pt and Te or Te oxides particles cannot be distinguished because of the similar darkness in TEM image. Fig. 3 depicts a sharp distribution of its metal particle size and its mean particle size is about 2.8 nm. The mean particle size is in good agreement with the XRD result. So, the method to prepare nanocatalyst is convenient and efficient.

The state of Te in Pt_3Te/C catalyst was then analyzed. TEM-EDX analysis was carried out in the center of catalyst particle and on the surface of carbon support where there was no catalyst particle. The analyzed points are shown as white and black cir-

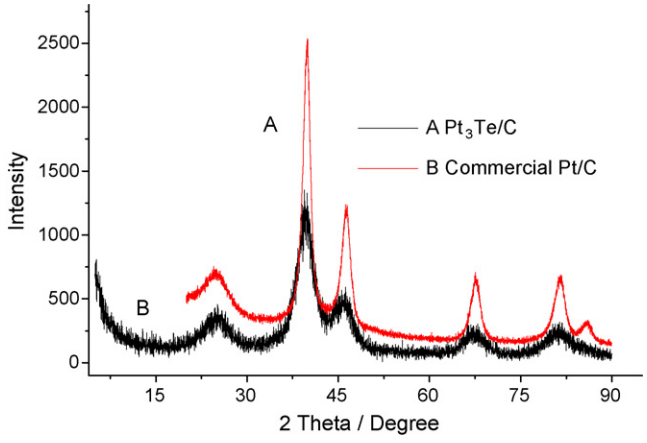

Fig. 1. XRD patterns of different catalysts: (A) commercial Pt/C; (B) synthesized Pt_3Te/C.

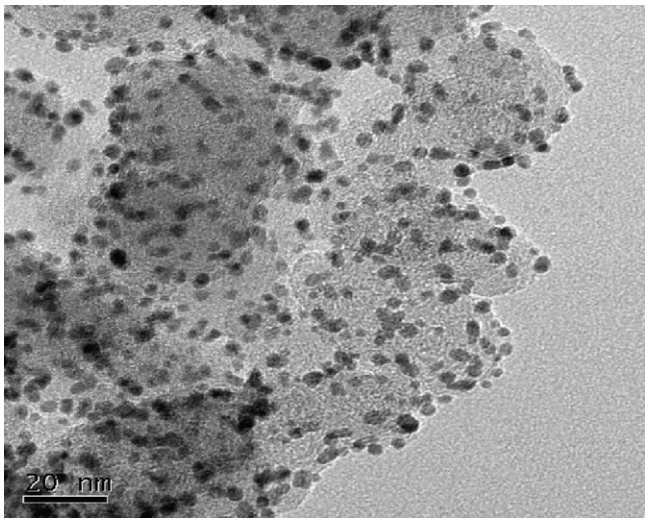

Fig. 2. TEM micrograph of the Pt_3Te/C catalyst.

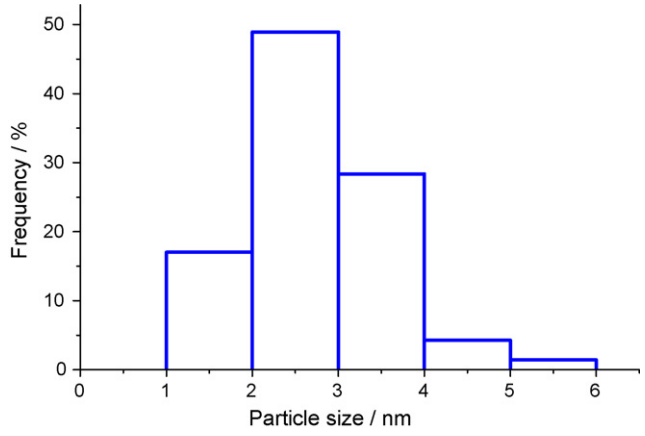

Fig. 3. A typical TEM image of the Pt_3Te/C particles size distribution.

cles in TEM image (Fig. 4). Pt and Te were not detected on the surface of carbon support (analyzed point C). On the contrary, Pt and Te are detected on the catalyst particles.

In order to know the electrochemical behaviour of the synthesized catalyst, the mass activity (A g^{-1}, MA), defined by peak

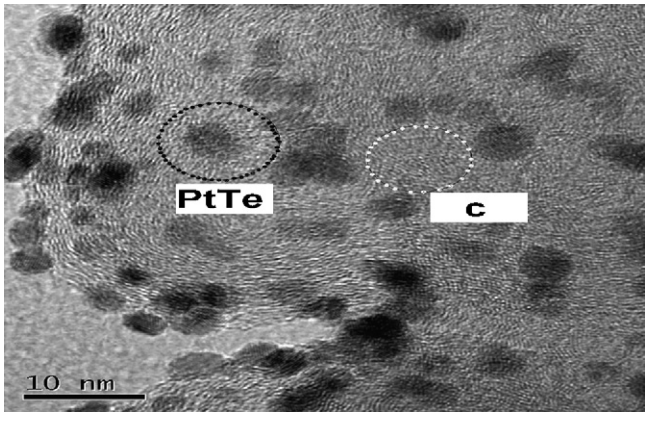

Fig. 4. TEM image of Pt_3Te/C catalyst in TEM-EDX analysis. White and black circles show the analyzed points by TEM-EDX.

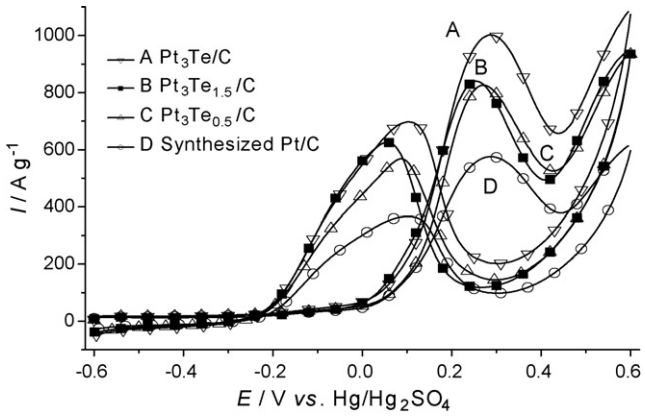

Fig. 5. The cyclic voltammograms of ethanol oxidation on different catalysts at 50 mV s^{-1} in 1 M C_2H_5OH + 0.5 M H_2SO_4. (A) Pt_3Te/C; (B) $Pt_3Te_{1.5}$/C; (C) $Pt_3Te_{0.5}$/C; (D) synthesized Pt/C.

current density (mA cm^{-2}, i_p) per the Pt loading mass (mg cm^{-2}, M), is used to evaluate the electrochemical activity of catalyst for ethanol oxidation in this paper, i.e. MA = i_p/M. Fig. 5 shows the cyclic voltammograms of ethanol oxidation for synthesized catalysts with different atomic ratios. Obviously, the addition of Te enhances the activity of Pt-based catalyst. The Pt_3Te_x catalysts have higher anodic current of ethanol oxidation than the Pt/C catalyst. And the Pt_3Te/C catalyst has the highest anodic peak current density while the Pt/C catalyst has the lowest anodic peak current density. At the same time, Fig. 6 shows the cyclic voltammograms of ethanol oxidation for synthesized Pt_3Te/C, commercial Pt/C and PtRu/C catalysts. It is observed that commercial Pt/C catalyst shows the most positive onset potential in the forward scan, and commercial PtRu/C and Pt_3Te/C have the same onset one. The forward scan peak potentials on Pt/C, PtRu/C and Pt_3Te/C are 250, 275 and 286 mV (versus MMS), respectively. It is interesting to find that in Fig. 6, the Pt_3Te/C has the highest anodic peak current density for ethanol electrooxidation among the catalysts investigated here. They are about 1002, 832, and 533 A g^{-1} for Pt_3Te/C, commercial PtRu/C and Pt/C, respectively. Here the ratio of the forward to reverse anodic peak current density, I_f/I_b, is used to describe the tolerance of

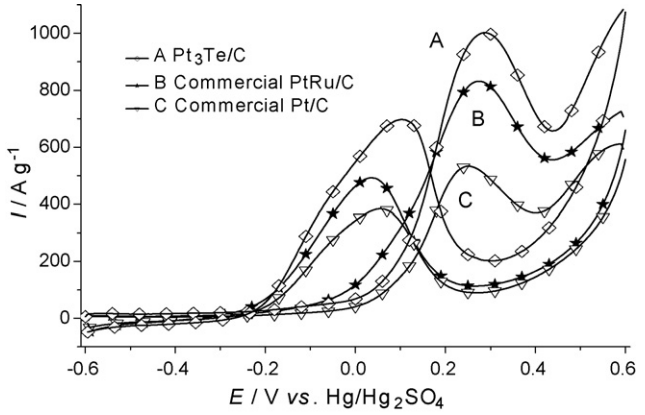

Fig. 6. The cyclic voltammograms of ethanol oxidation on different catalysts at 50 mV s^{-1} in 1 M C_2H_5OH + 0.5 M H_2SO_4. (A) Commercial PtRu/C; (B) commercial Pt/C; (C) Pt_3Te/C.

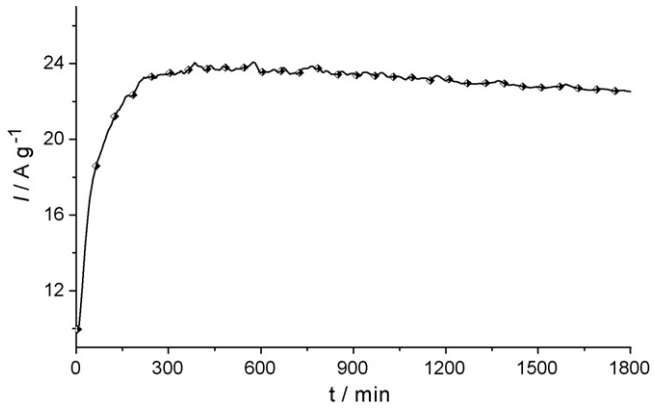

Fig. 7. Current–time curves of Pt_3Te/C catalyst in 1 M C_2H_5OH + 0.5 M H_2SO_4 at 0.5 V versus RHE.

the catalyst to the accumulation of carbonaceous species. A low I_f/I_b ratio indicates poor oxidation of ethanol to carbon dioxide during the anodic scan, and excessive accumulation of carbonaceous residues on the catalyst surface. A high I_f/I_b ratio shows the converse case [21,22]. From the results given in Fig. 6, their ratios are 1.39 for Pt/C, 1.69 for PtRu/C and 1.44 for Pt_3Te/C. So the anti-poisoning ability has the following order: PtRu/C > Pt_3Te/C > Pt/C. The PtRu/C has a better anti-poisoning ability than the Pt_3Te/C.

The average size of the commercial catalysts (Pt/C and PtRu/C) has been reported. The average size of Pt/C obtained from XRD peak and TEM image is 2.6 and 2.7 nm, respectively, and for PtRu/C, it is 2.4 and 2.7 nm [23]. And the particle size of the Pt_3Te/C nanoparticles synthesized in our work is 2.4 (XRD) and 2.8 nm (TEM). This implies that the specific surface area of Pt in the Pt_3Te/C nanocatalyst is approximately the same as that of Pt in the commercial catalysts. Compared to the Pt_3Te_x/C catalysts, the synthesized Pt/C catalyst has the lowest anodic peak current density. So, from the viewpoint of current, Te makes the Pt_3Te/C nanocatalyst have higher activity for ethanol electro-oxidation. The superior activity of the Pt_3Te/C electrocatalyst may be attributed to the electronic modification of platinum or the presence of Te oxide species, which may play the role of electronic effect or bifunctional mechanism [24–26].

The Pt_3Te/C eletrocatalyst performance for ethanol oxidation was also studied by chronoamperometry in 1 M C_2H_5OH + 0.5 M H_2SO_4 solution at 0.5 V versus reversible hydrogen electrode (RHE) and its current–time curve is shown in Fig. 7. The current values were normalized per gram of platinum, considering that ethanol adsorption and dehydrogenation occur only on platinum sites at room temperature. Fig. 7 shows that the current increases quickly in the initial 240 s, then it drops slowly. It is found that the current values obtained for Pt_3Te/C eletrocatalyst were higher than those reported [27–29].

4. Conclusions

Due to its high stability in acidic solution and cheapness, Te as a non-metallic element was selected for the first time as the second element of the Pt-based catalyst for ethanol electro-oxidation in sulfuric acid solution. The Pt_3Te/C nanocatalyst was successfully prepared and it shows the highest anodic peak current density for ethanol electro-oxidation among the Pt_3Te_x catalysts with different atomic ratios. And the Pt_3Te/C catalyst also has higher anodic peak current density than the commercial Pt/C and PtRu/C catalysts. Up to date, in the view of peak current density, the Pt_3Te/C nanocatalyst is the best binary catalyst for ethanol electro-oxidation [27–29,30–32]. This implies that the Pt_3Te/C nanocatalyst may be a good candidate for ethanol electro-oxidation. Its synthesis is also convenient and efficient for producing nanocatalyst. This finding may be helpful for the development of fuel cell for its high activity and cheapness. But the anti-poisoning ability still needs to be improved and the mechanism study is still in progress.

Acknowledgment

This research was partially supported by the Natural Science Foundation of Fujian Province of China (No. 2006J0272).

References

[1] A.O. Neto, E.G. Franco, E. Aricó, M. Linardi, E.R. Gonzalez, J. Eur. Ceram. Soc. 23 (2003) 2987.
[2] C. Lamy, A. Lima, V. Lerhum, F. Delime, C. Coutanceau, J.M. Léger, J. Power Sources 105 (2002) 283.
[3] A.O. Neto, R.R. Dias, M.M. Tusi, M. Linardi, E.V. Spinacé, J. Power Sources 16 (2007) 87.
[4] E.V. Spinacé, A.O. Neto, M. Linardi, J. Power Sources 129 (2004) 121.
[5] A.L.N. Pinheiro, A.O. Neto, E.C. Souza, E.A. Ticianelli, J. Perez, E.R. Gonzalez, J. New Mat. Electrochem. Systems 6 (2003) 1.
[6] T. Iwasita, Electrochem. Acta 47 (2002) 3663.
[7] E.V. Spinacé, A.O. Neto, M. Linardi, J. Power Sources 124 (2003) 426.
[8] F. Vigier, C. Coutanceau, F. Hahn, E.M. Belgsir, C. Lamy, J. Electroanal. Chem. 563 (2004) 81.
[9] C. Lamy, E.M. Belgsir, J.M. Léger, J. Appl. Electrochem. 31 (2001) 799.
[10] G.A. Camara, R.B. Lima, T. Iwasita, Electrochem. Commun. 6 (2004) 812.
[11] G.C. Li, P.G. Pickup, Electrochim. Acta 52 (2006) 1033.
[12] E. Antolini, F. Colmati, E.R. Gonzalez, Electrochem. Commun. 9 (2007) 398.
[13] F.C. Simóes, D.M. Anjos, F. Vigier, J.M. Léger, F. Hahn, C. Coutanceau, E.R. Gonzalez, G.T. Filho, A.R. Andrade, P. Olivi, K.B. Kokoh, J. Power Sources 167 (2007) 1.
[14] F. Colmati, E. Antolini, E.R. Gonzalez, J. Power Sources 157 (2006) 98.
[15] F. Vigier, C. Coutanceau, A. Perrard, E.M. Belgsir, C. Lamy, J. Appl. Electrochem. 34 (2004) 439.
[16] A.O. Neto, M.J. Giz, J. Perez, E.A. Ticianelli, E.R. Gonzalez, J. Electrochem. Soc. 149 (2002) A272.
[17] C.W. Xu, S.P.K. hen, X.H. Ji, R. Zeng, Y.L. Liu, Electrochem. Commun. 7 (2005) 1305.
[18] B. Liu, J.H. Chen, X.X. Zhong, K.Z. Cui, H.H. Zhou, Y.F. Kuang, J. Colloid Interface Sci. 307 (2007) 139.
[19] L.H. Jiang, Z.H. Zhou, W.H. Li, W.J. Zhou, S.Q. Song, H.Q. Li, G.Q. Sun, Q. Xin, Energy Fuels 18 (2004) 866.
[20] C. Roychowdhury, F. Matsumoto, V.B. Zeldovich, S.C. Warren, P.F. Mutolo, M. Ballesteros, U. Wiesner, H.D. Abruna, F.J. Disalvo, Chem. Mater. 18 (2006) 3365.
[21] Z.L. Liu, X.Y. Ling, X.L. Su, J.Y. Lee, L.M. Gan, J. Power Sources 149 (2005) 1.
[22] Z.L. Liu, L. Hong, J. Appl. Electrochem. 37 (2007) 505.
[23] W.J. Zhou, W.Z. Li, Z.H. Zhou, S.Q. Song, Z.B. Wei, G.Q. Song, P. Tsiakaras, Q. Xin, Chem. J. Chin. Univ. 24 (2003) 858.
[24] E.V. Spinacé, M. Linardi, A.O. Neto, Electrochem. Commun. 7 (2005) 365.

[25] J.H. Choi, K.W. Park, B.K. Kwon, Y.E. Sung, J. Electrochem. Soc. 150 (2003) A973.
[26] K.W. Park, J.H. Choi, S.A. Lee, C. Pak, H. Chang, Y.E. Sung, J. Catal. 224 (2004) 236.
[27] A.O. Neto, R.R. Dias, M.M. Tusi, M. Linardi, E.V. Spinaé, J. Power Sources 166 (2007) 87.
[28] H.Q. Song, X.P. Qiu, F.S. Li, W.T. Zhu, L.Q. Chen, Electrochem. Commun. 9 (2007) 1416.
[29] H.Q. Song, G.Q. Sun, L. Cao, L.H. Jiang, Q. Xin, Electrochim. Acta 52 (2007) 6622.
[30] H.Q. Song, X.P. Qiu, X.X. Li, F.S. Li, W.T. Zhu, L.Q. Chen, J. Power Sources 170 (2007) 50.
[31] Y.X. Bai, J.J. Wu, X.P. Qiu, J.Y. Xi, J.S. Wang, J.F. Li, W.T. Zhu, L.Q. Chen, Appl. Catal. B 73 (2007) 144.
[32] Y.X. Bai, J.F. Li, X.P. Qiu, J.J. Wu, J.S. Wang, J.Y. Xi, W.T. Zhu, L.Q. Chen, J. Mater. Sci. 42 (2007) 4508.